ISSN 2347-3487

LOW PRESSURE CH_2Cl_2PLASMA DISCHARGE

J. C. Poveda, O. Flores, H. Martinez, B. Campillo and F. B. Yousif.
Escuela de Química, Facultad de Ciencias, Universidad Industrial de Santander Bucaramanga, Santander, Colombia A.A. 678.
jkclimb@hotmail.com
Instituto de Ciencias Físicas, Universidad Nacional Autónoma de México, Apartado Postal 48-3, 62251, Cuernavaca, Morelos, México.
osvaldo@fis.unam.mx; hm@fis.unam.mx
Facultad de Química-Instituto de Ciencias Físicas, Universidad Nacional Autónoma de México, Av. Universidad 1000, México, D. F. México.
bci@fis.unam.mx
Centro de Investigación en Ciencias, Universidad Autónoma del Estado de Morelos.
fbyousif@uaem.mx

ABSTRACT

Glow discharge of dichloromethane (DCM) was investigated employing Optical Emission Spectroscopy (OES), while the electron temperature and electron densitywere measured using a double Langmuir probe. Deposits formed were characterized by Scanning Electron Microscopy (SEM), X-ray Photo Fluorescence Spectroscopy (XPS) and Fourier Transform Infrared Spectroscopy (FTIR). The species identified by OES were the molecular bands of C_2, C_3, CH, H_2, CH^+, HCl^+, Cl and C^+. The material deposited displays a growing behavior. SEM observation shows several features which correspond to coalesce and growth mechanism. The characterization of the material deposited can explain the different stages of deposits that are formed on the electrode surface. Several factors are concerned in the complexity of the process, regarding the interaction of species formed during the plasma discharge. Involving several bonds types such as: C=C, C=C-CH_2-Cl, C-C and CH.

Indexing terms/Keywords

CH_2Cl_2, low pressure plasma, low temperature plasma

Academic Discipline And Sub-Disciplines

Experimental physics, low temperature physics, plasma physics; particle beam interactions in plasmas, optical (visible, infrared) measurements, plasma-based ion implantation and deposition, electric discharges, discharge in solids.

SUBJECT CLASSIFICATION

American Institute of physics.

TYPE (METHOD/APPROACH)

Experimental research.

INTRODUCTION

From a technological point of view, there has been increasing interest in the use of glow discharges as an efficient method for the polymerization of a number of organic[1], organometallic compounds[2, 3], and metal oxide deposition[4]. On the other hand, anthropogenic emissions results in the increment of chemical species, which are easily ionized in the upper atmosphere. One of the chemical species that are highly reactive is the halogenated compound, known as one of volatile organic compounds (VOC's). This compound is ionized as it interacts with vacuum ultraviolet light and UV photons, leading the formation of neutral and ionized species. In exploring the intermediate species produced in low-temperature plasmas, one can contribute significantly to understanding the chemical and physical processes taking place in the atmosphere. Some of these VOC's can be produced through specific technological applications [5], including atmospheric pressure plasmas [6, 7]. Equally, it has been well recognized that several industrial process release an increasing amounts of VOC's into the environment, together with their potential detrimental health effects[8]. These VOC'sinclude the chlorinated compounds such as trichloroethylene, tetrachloroethylene and dichloromethane (DCM) used as solvents in various chemical and polymer syntheses and degreasing operations. However non-thermal plasma technique has been applied to the decomposition of DCM [9,10]. This may proceed through the process of initiation, propagation, and completion of the involved reactions. Several mechanisms are involved leading to chain reactions and generation of radicals. However, VOC's molecules will propagate until stable compounds are formed. The ideal products of decomposition of toxic compounds are CO_2, H_2O, and HCl for organic chlorides. Furthermore, since the plasma generated radicals reactions are difficult to control as previous investigations showed that some toxic byproducts are inevitably formed during the decomposition of some VOC's[11], which may cause additional environmental pollution. Therefore, it is essential to inhibit the production of secondary pollutants in order for this technology to be applied to practical applications. So far, there have been no experimental or theoretical studies dealing with the deposition of solid products coming from the decomposition of the DCM.

EXPERIMENTAL

The experiments are performed employing a parallel plate reactor as seen in figure 1.The DC plasma emission devicesare well described elsewhere [12,13]. Pure Cu 99.99% substrates (1 mm thick and 30 mm in diameter) were used for the deposition of DCM; the Cu substrates were degreased, rinsed thoroughly and dried. An ultra-pure DCM (spectroscopy 99.99 purity) was used throughout the experimental work. The duration of depositions was between 0 and 45 min. The DCM flow rate of 12 l/min was maintained. The base pressure of the plasma chamber of $2.0x10^{-3}$ Torr, was reached employing a mechanical pump and Ar gas was used to purge the vacuum chamber. The DCM plasma was pulsed (60 Hz)at1.0 Torr pressure. The plasma discharge was maintained by a voltage of 800 volts and a current I_D of 25 mA. The glow discharge was monitored by plasma emission spectroscopy through a quartz window installed on the right lateral flange with an optical fiber positioned at the center of the window in order to collect the light emitted by the plasma. The characteristics of the spectrometer are well described previously [12]. A double Langmuir probe was inserted between the two electrodes. The probe current was monitored as the probe voltage was manually varied from +30 V to -30 V. The *I-V* measurement time was between 5 to 10 minutes. The *I-V* curve reported here is a summary of six data scans, which are used to determine the electron temperature (T_e) and electron density (n_e). The deposits mass (m_L) was determined by the electrode mass before and after the deposition process.

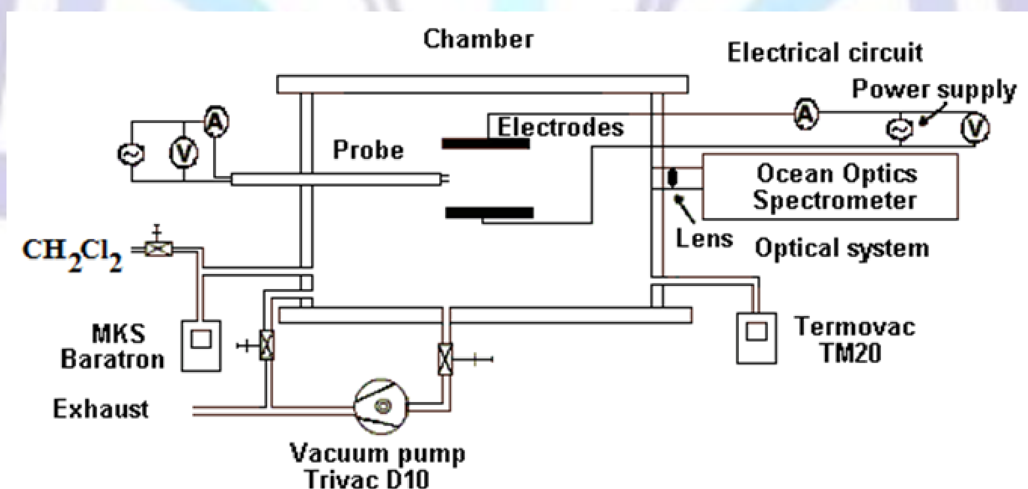

Fig 1: Experimental apparatus

Scanning Electron Microscopy (SEM) observations were performed employing a JEOL JSM 5900LV microscope equipped with an energy-dispersive X-ray detector. X-ray diffraction (XRD) measurements were made with a Rigaku Dmax-2200 diffractometer, using monochromatic high-intensity Cu Kα radiation (λ=1.542 Å) and operating at 36 kV and 30 mA, with a 2θ scan range between 5° and 40°. The XPS analysis were done in a CAMECA MAC 3©, XPS-AES system. A survey scan and high resolution scans using XPS of the C(1s), Si(2p), and O(1s) regions were obtained for all the samples. The X-ray source of CAMECA system produces two kinds of X-ray lines with energies hν(Mg-Kα) 1253.6 eV and hν(Al-Kα)= 1486.6eV. Fourier transform infrared (FTIR) was used to measure the attenuated total reflectance (ATR), in the mid-IR

ISSN 2347-3487

region of 500-4000 cm^{-1}. 50 mg of MD was located at the ATR crystal spectrometer used. The XPS scans are done using photons with an energy of $h\nu$ (AlKα) =1486.6 eV. This technique is particularly sensitive in distinguishing several carbon phases and carbides present in the film. The energy resolution in the spectra was found to be 1.2 eV for XPS, evaluated from thefull width at half-maximum intensity(FWHM) value of C(1s) peak.

RESULTS AND DISCUSSION

Electron temperature and electron density measurements

The procedure used to determine T_e and n_e has been previously described [12,13]. This procedure gave an electron temperature of T_e = (5.47 ± 0.27) eV and an electron density of n_e=(1.57±0.06) x 10^{16} m^{-3}. In this experiment, the probe radius of 0.5 mm, which is larger than the Debye length of λ_D=0.14 mm, meeting the condition that is needed for the transition sheath region (TSL) [14]. The main error involved in analyzing the data is due to the inaccuracy of the measurements of probes areas. Typical differences in both sides of the saturation regions of the I-V curve produces slightly different slopes leading to an error in the electron temperature. The experimental error of 5% for the electron temperature and 4% in the electron density values were calculated.

Optical Emission Spectroscopy (OES) measurements

Figure 2, shows the present measurements of the OES of the DCM glow discharge. The spectra allowed analysis of the most luminous area, which corresponds to the negative glow near the cathode dark space. Observed emission lines and bands of the discharge were assigned as indicated in table 1[15]. The integration time and the fiber optics position were fixed. The principal signals identified in the OES were from the molecular bands of $C_2(c'^1\Pi_g-b^1\Pi_u)$, $C_3('\Pi_u-'\Sigma^+_g)$, $CH(A^2\Delta-X^2\Pi)$, H_2, $CH^+(A'\Pi-X'\Sigma)$, $HCl^+(A^2\Sigma-X^2\Pi)$, as well as those of Cl and C^+. The absence of the H is probably due to the fact that the production of $CH(A^2\Delta-X^2\Pi)$, $CH^+(A'\Pi-X'\Sigma)$, $HCl^+(A^2\Sigma-X^2\Pi)$ signals may inhibit the H and H_2 signals.

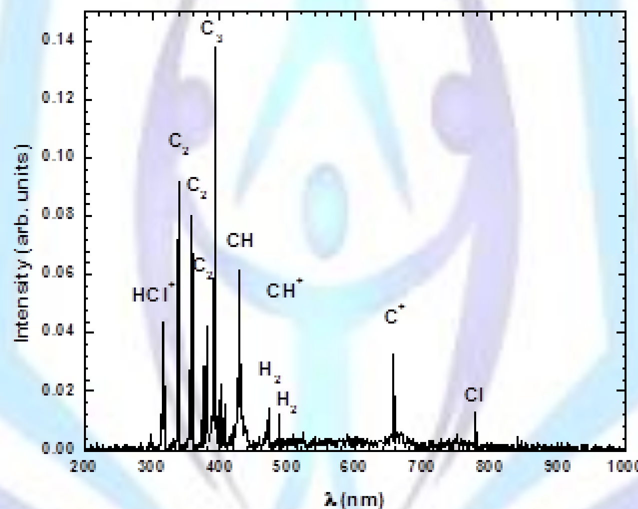

Fig 2: Emission spectra of DC plasma discharge of CH_2-Cl_2.

Table 1. Table captions should be placed above the table

Species	Transition wavelength, nm
$C_2(c'^1\Pi_g-b^1\Pi_u)$	339.61, 358.60 and 377.96
$C_3('\Pi_u-'\Sigma^+_g)$	392.50
$CH(A^2\Delta-X^2\Pi)$	431.42
Cl	778.28
C^+	657.80
H_2	471.90 and 487.30
$CH^+(A'\Pi-X'\Sigma)$	380.61
$HCl^+(A^2\Sigma-X^2\Pi)$	317.73

Mass deposition (MD)

The MD on the lower electrode as seen in figure 3 was identified as a yellow-orange layer and is shown as a function of the discharge time. Three stages can be depicted:

a) The MD shows a small increasing behaviour during the first 15 min, with a deposition rate of about 0.3 mg/min;

b) between 15 min and 30 min, in which the MD display a strong increasing behaviour, with an approximated growth rate of 1.0 mg/min; and

c) after 30 min of discharge time, the MD indicates a saturation behavior. This behavior suggests that the DCM was consumed producing these deposits.

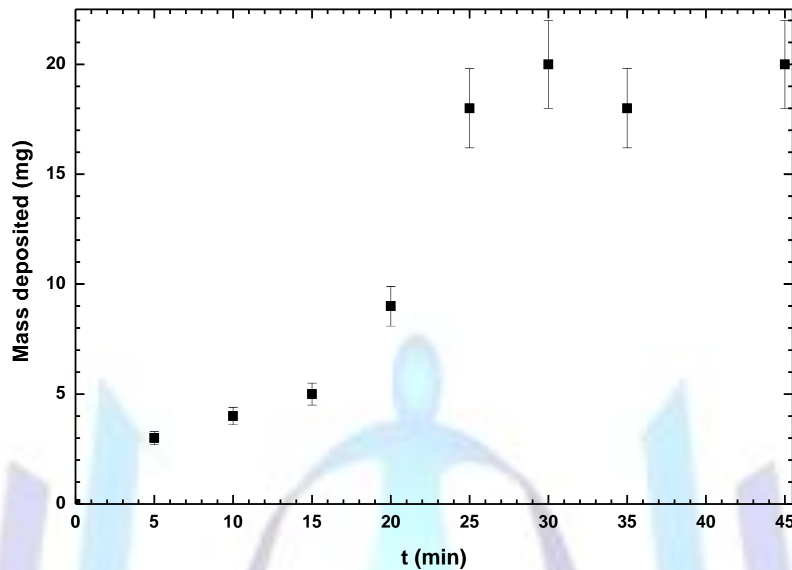

Fig 3: Mass deposited on the electrode as a function of discharge time.

SEM and XRD observations

The surface morphology was carried out by SEM analysis. Figures 4(a) to 4(c) show the SEM surface images of the MD on the Cu substrate after being exposed to DC plasma discharge of DCM at 5, 10 and 30 min, respectively. By increasing the exposure time, several features dispersed on the Cu surface can be seen.

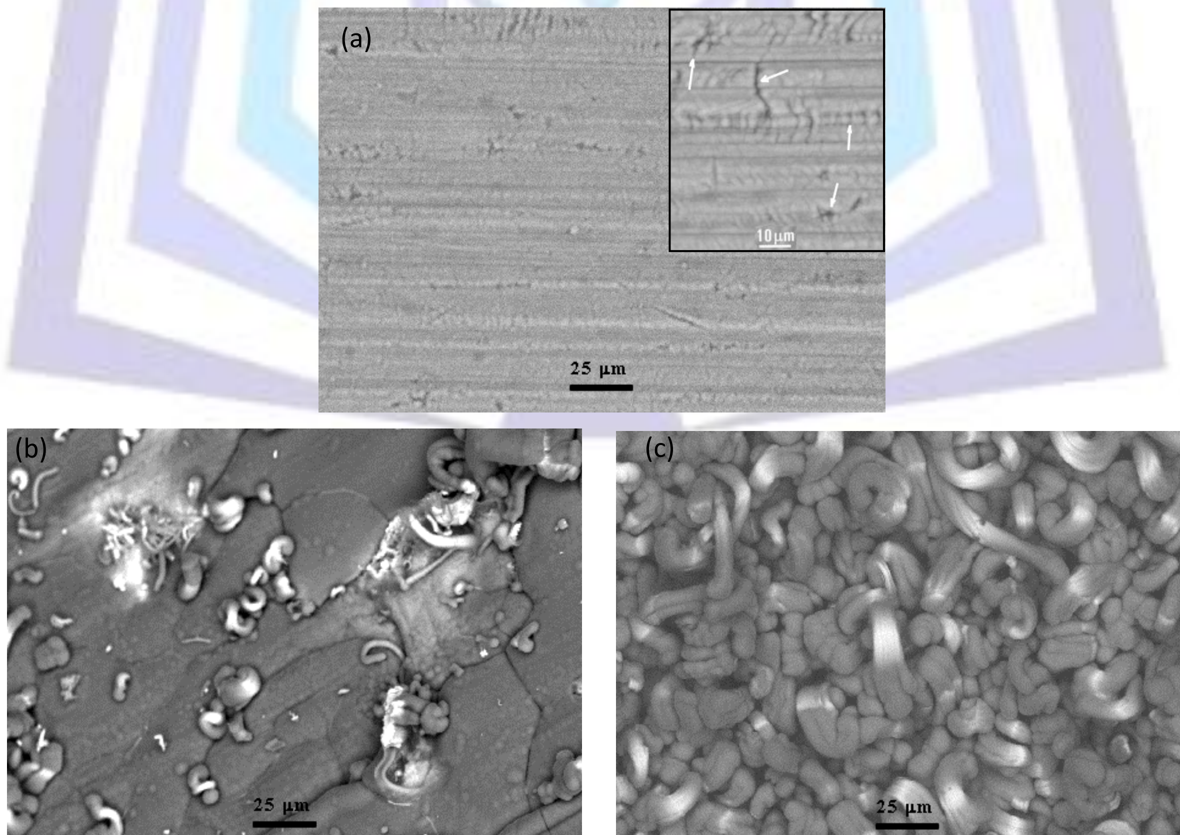

Fig 4: SEM micrographs : a) at 5 min of discharge time; b) at 10 min of discharge time ; c) at 30 min of discharge time.

ISSN 2347-3487

A very fine discontinuous layer adhered to the Cu substrate was formed at 5 minutes exposure time and no-particle like morphology were recognized as shown in figure 4(a). These discontinuous layers are more like fibrillar objects with pits and fissures (see arrows on insert in figure 4.a). In figure 4b, after 10 minutes exposure time, the appearance of twisting worm-like features is evident and starts to form on top of the film layer already formed with an average size of 3.5 μm in width and in an average length of 8.5 μm. An increase in the size and volume of these features is observed after 30 minutes exposed time; their sizes ranging from 8 to 12 μm in width and 20 to 30μm in length, as shown in figure 4c. From these observations, the worm-like twisted features after 30 min discharge time seem to be connected to each other with the appearance of coalescence of two or more individual features. These observations suggest that these worm-like features are residues. Similar morphologies observed [16] were related to globular and worm-like crystals that are coming from the epitaxial growth of edge-on fashion. The changing deposit/Cu surface interactions alongside the decomposition process, affects the observed morphology as the discharge time increases and possibly saturates the growth of crystals due to fewer periods for molecule/substrate interaction. It can be said that the DCM can suffer several intrinsic reactions such as decomposition and dissolution in order to contribute to the formation of such morphology.

The structural properties of the MD were investigated employing XRD. Figure 5 shows the diffraction patterns for 5, 15 and 30 min discharge times. The XRD patterns of all samples were similar, and showed narrow and sharp peaks. All treated samples showed three sharp peaks observed at 28.5°, 47.40° and 56.34° respectively, corresponding to the crystal structure of nantokite phase [17], and also two peaks can be observed arising from the metallic Cu substrate at 43.34º and 50.46°. However, one sharp peak at 36.36° was observed only at the 5 minutes treatment time, corresponding to the compound phase of the CuCl-crystal structure. Although, in increasing the treatment time, this CuCl phase does not continue to form. This would suggest that the DCM decomposition time is short. At longer treatment time, the efficiency of its decomposition decreases. This behaviour was presumed to be caused by chemisorption of DCM radicals onto the surface of the Cu-substrate[18] . On the other hand, the nature of the plasma and the surface-species generated may contribute to the decrease of decomposition as the treatment time is increased. The reaction mechanism involved has been previously outlined using air or nitrogen plasma [9, 10], and the present results are in agreement with the study performed.

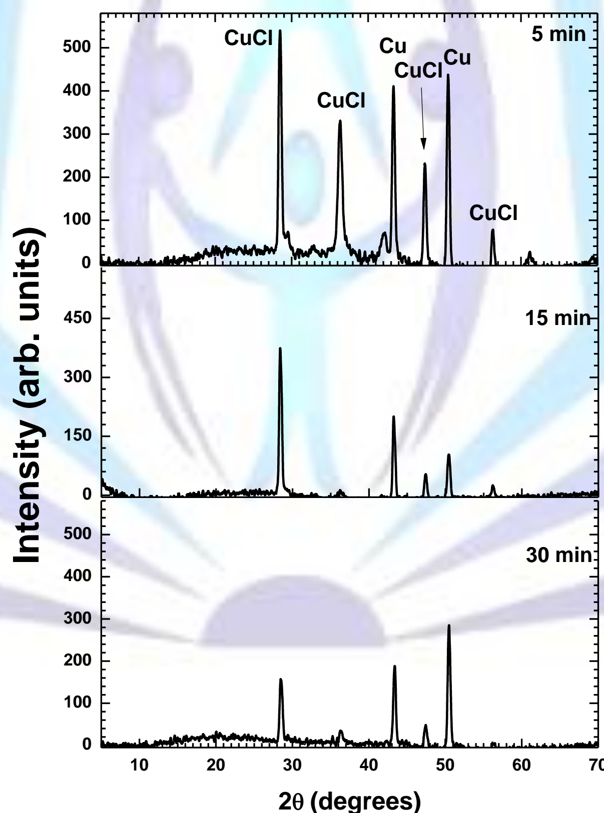

Fig 5: XRD patterns.

FTIR analysis of material deposits.

FTIR spectroscopy was used to analyze the surface of the MD. Figure 6 shows the FTIR spectra for the untreated sample (pristine) of MD produced in DCM plasma discharge for 5, 15 and 30 minutes. Fewer bands in the IR spectra are observed as the residence time of DCM in the plasma was increased. Within the discharge, neutral radicals formed occur due to the dissociation of DCM. Radicals can react with each other, thus giving more complex structures through a step by step mechanism, leading to increased particle size as the discharge time increases. From the IR spectra, the observation of fewer bands in the IR spectra points out to the presence of only few chemical species that are involved, increasing the C-C bonds and removing Cl and H atoms from the thin film. The IR spectra of figure 6 identifies signals at 3400-3300 cm^{-1},

and are assigned to a C-H stretching joined to *sp* carbon. The C-H has sp^3 that is observed at 3500 cm^{-1}, while other bands display a less structure shape as the discharge time increases (see figure 6 at 30 min). The *sp*-*sp* carbon signal was observed at 2180 cm^{-1}. The C-H stretching signal at 2010 cm^{-1} is observed when C-H atoms in sp^2 configuration are binding to a second sp^2 carbon atom. At 30 min of plasma discharge (figure 6), the signals were completely lost. Signals observed at 1580 cm^{-1} are identified as sp^2-sp^2 carbons stretching bond joined to Cl atoms as $C=CCl_2$. The signals at 1120 cm^{-1} correspond to sp^3-sp^3 carbon bonds bending, which also is assigned to $-CH_2Cl$ fragment. Signal at 1030 cm^{-1} correspond to C-Cl stretching bond and the 620 cm^{-1} signal is related to a deformation of the C=C-Cl. As the reaction time increases, the structural fragment that includes Cl was lost. That behavior can be correlated with the Cl signal observed in optical emission spectroscopy. From SEM observation, an increase in the particle size was observed, which gives support to the decreasing intensity of the stretching bands, containing chlorine atoms observed in the IR spectra due to the chemical interaction.

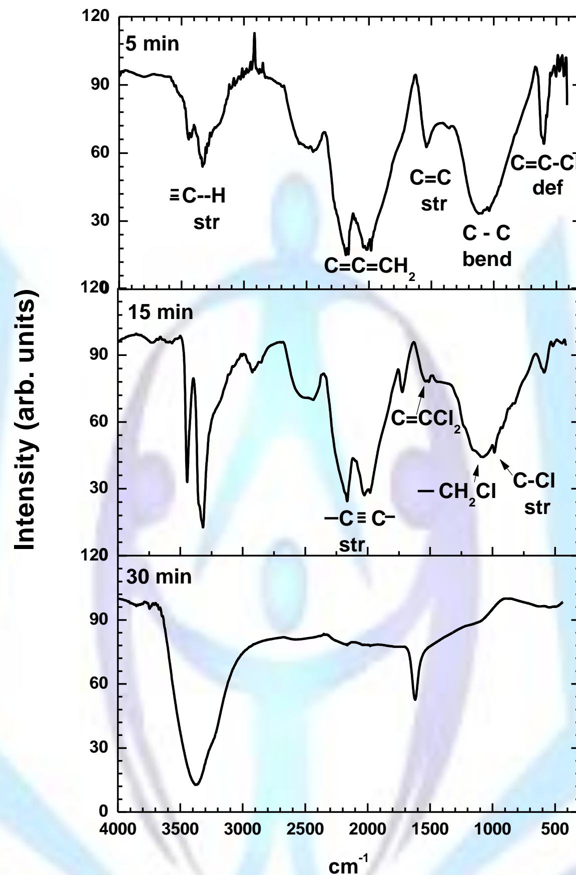

Fig 6: IR spectra of MD.

The signals attributed to Cu-Cl were not observed in the FTIR analysis, since they are observed around 108, 302 and 407 cm^{-1}. Furthermore, vibrational strength of Cu-Cl bond can be detected in the range of 600-800 cm^{-1}, but they overlapped with the C=C-Cl signal, which decreases as the reaction time is increased, for being attributed to a progressive replacement of the chlorine atom by the radical CH_2Cl. This phenomenon is used to explain the morphology of the deposit seen in the SEM images (see figure 4).

XPS analysis.

XPS spectra were applied to surface analysis. XPS spectra of the MD on the electrode at 5, 15 and 30 minutes discharge time are shown in figure 7.

In order to have better understanding of the element composition of the MD on the electrode, we have used a quantitative analysis. The general expression for determining the atom fraction of any constituent in a sample, C_x, can be written as:

$$C_x \approx \frac{n_x}{\sum n_i} \approx \frac{I_x/S_x}{\sum I_i/S_i}$$

where, C_x is the atom fraction; n_x, is the number of the atoms of the element; I_x, is the number of the photoelectrons per second (area under the curve) from the element; I_i, is the sum of all Intensities from all elements in the constituent; S_x, is the sensitivity factor, and S_i is the sum from all elements in the constituent. In table 2, the atomic fraction of the elements C 1s and Cl 2p are listed. We observe that the atomic fraction of the C decrease, while the atomic fraction of Cl increase as the discharge time increase.

ISSN 2347-3487

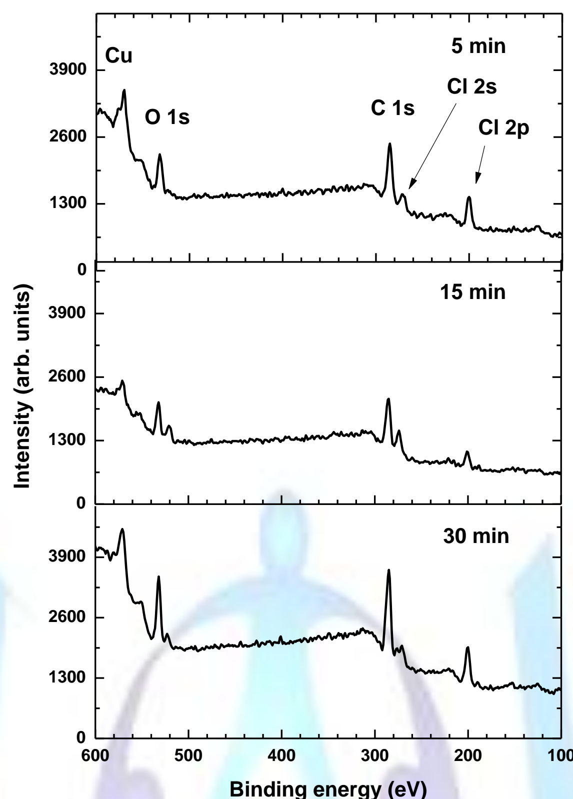

Fig 7: XPS spectra of MD.

Table 2. Table captions should be placed above the table.

Sample	Atomic Fraction	
	C 1s region	Cl 2p region
CH_2Cl_2 5 min.	0.9	0.1
CH_2Cl_2 15 min	0.8	0.2
CH_2Cl_2 30 min	0.7	0.3

DISCUSSION

In the present DC plasma discharge of DCM several possible reactions may occur yielding a variety of chemical species. The kinetics may involve several different chemical species: electrons (e^-), positive ions (C^+), radicals (CH), atoms (Cl, C) and molecules (C_2, C_3, H_2, CH_2, HCl and CH_2Cl). The DCM dissociation takes place along the C-Cl bond, leading to free chlorine atoms [19] observed by OES. Equally, the detection of neutral molecules such as C_2 and C_3, reveals the probability of higher collision frequencies. Considering the experimental conditions (V=800 Volts, d=10 mm, P= 1 Torr) and taking T_g= 400 K, the electron density (CH_2Cl_2) of n_e=1.57x10^{16} m^{-3} (assuming n_i=n_e), we calculated an ionization degree of ~10^{-7} which is lower than 10^{-4}, therefore, the electron-electroninteraction can be ignored [20]. As the I_D is 25 mA and the area of electrode is 7.07 cm^2 , hence we can set the plasma ion flux to ~3.41x10^{22} m^{-2} min^{-1}. This ion flux heats the electrodes, which can explain the activation of CuCl (confirmed by XRD and XPS observations). This promotes the growth of the central chain which is attached by physisorption process to the copper surface electrode, as it can be observed in the micrographs (figure 4). The FT-IR experiments showed that the Mass depositions MD are formed chemically by structural type CH, CC, C = C, C = C-CH_2-Cl and Cl.Moreover, XRD experiments showed the formation of phases of Cu-Cl type, possible formed during the first stage of the of surface activation and their relative content progressively decreases with discharge time, as can be seen by comparing the spectra's at 5, 15 and 30 min (figure 5).These may indicate that the active centers of surfaces electrode are progressively replaced by neutral species of the type CH_2 or CH^{2+}. Thus showing a growth mechanism of the central chain by adding more units of CH_2 and forming a linear chain, which increases in time, as it is demonstrated in the XPS experiments.At the earliest stage, the MD only promotes the growth of single central chains, composed mainly by carbon, hydrogen and small amount of chlorine, thus, observing a C:Cl ratio of 9:1 at 5 min of time deposition. As the deposition time increases, the XPS results of figure 4 shows that the chlorine content increases gradually with respect to carbon as the chlorine atoms are gradually incorporated in the backbone chain, which is increasing, as seen from the XPS data at 10 and 30 min of time deposition. This would indicate the presence of an

additional stage characterized by the addition of CHCl type fragments to the chain centers in which the hydrogen atoms are replaced by chlorine atom.

This substitutional process in the last stage of growth is limited by steric effects due to the size of the chlorine atoms.Since the growth and replacement are not controlled and they are randomized, it is not possible to propose a basic structure to explain the composition of the monomer and tacticity of the deposits. For long treatment time, we might expect that the atomic composition of the sample is of the type $-(CHCl)_n-$ or $-(CH_2-CCl_2)_n-$ with atomic ratios 1:1, 2:2, respectively, for a partial substitution processes or the type $-(CCl_2)_n-$, $-(CHCl-CCl2)_n-$ or $-(CCl_2-CCl_2)_n-$ for processes of total saturation, with atomic ratios 1:2, 2:3 and 2:4, respectively.

From the plasma parameters such as density of radicals, temperature of electrons and charged particles, as well as in combination with analytical techniques, it is possible to control the deposited material.

CONCLUSIONS

Conclusions can be summarized as follows:

The principal signals present in the OES were from the molecular bands of $C_2(c'^1\Pi_g-b^1\Pi_u)$, $C_3('\Pi_u-'\Sigma^+_g)$, $CH(A^2\Delta-X^2\Pi)$, H_2, $CH^+(A'\Pi-X'\Sigma)$, $HCl^+(A^2\Sigma-X^2\Pi)$, Cl and C^+.

The MD shows an increasing behaviour during the first 30 min, with a growth rate of 87.93 mg/min. After 30 min of discharge time, the MD displays saturation behaviour during thin film formation. SEM observation shows several features which correspond to coalesce and growth mechanism.

The analysis by OES, SEM, FT-IR, XRD and XPS analysis can explain the different stages of deposits that are formed on the electrode surface. Several factors are concerned in the complexity of the process, regarding the interaction of species formed during the plasma discharge. That involves several chemical processes.

ACKNOWLEDGMENTS

The authors are grateful to F. Castillo, I. Puente, M. L. Ramón and H. H. Hinojosa for technical assistance and to Dr. L. Cota-Araiza for helpful discussion. This research was partially sponsored by DGAPA IN-105010, CONACyT 225991.

REFERENCES

[1] Cho, S. J., Bae I. S., Boo, J. H., Park, Y. S., Hong, B. 2008.Study on the plasma-polymer thin films deposited by using PECVD and application tests for low-k insulator. J.Korean Phys. Soc. 53, 1634-1637.

[2] Shah Jalal, A. B. M., Ahmed, S., Bhuiyan, A. H., Ibrahim, M. 1996.UV-Vis absorption spectroscopic studies of plasma-polymerized m-xylene thin films.Thin Sol. Films,288, 108-111.

[3] Dilsiz, N., Akovali, G. 1996.Plasma polymerization of selected organic compounds.Polymer. 37 (2), 333-342.

[4] Bae, S. J., Cho, S. H., Lee, S. B., Kim, Y. and Boo, J. H. 2005. Growth of plasma-polymerized thin films by PECVD method and study on their surface and optical characteristics. Surf. & Coat. Technol. 193, 142-146.

[5] Giardini, A., Marotta, V., Morone, A., Orlando, S. and Parisi, G. P. 2002.Thin films deposition in RF generated plasma by reactive pulsed laser ablation.Appl. Surf. Sci. 197-198, 338-342.

[6] Conrads, H., Schmidt, M. 2000. Plasma generation and plasma sources. Plasma Sources Sci. Technol. 9 (2000), 441-454.

[7] Selwyn, G. S., Herrmann, H. W., Park, J., Henins,I. 2001.Materials processing using an atmospheric pressure, RF-generated plasma source.Contrib. Plasma Phys. 6 (2001), 610-619.

[8] Vandenbroucke, A. M., Morent, R., De Geyter, N., Leys C, 2011. Non-thermal plasmas for non-catalytic and catalytic VOC abatement. J. of Haz. Mat. 195 (2011), 30-54.

[9] Fitzsimmons, C., Ismail, F., Whitehead, J. C., Wilman, J. J. 2000. The chemistry of dichloromethane destruction in atmospheric-pressure gas streams by a dielectric packed-bed plasma reactor. J. Phys. Chem. A. 104, 6032-6038.

[10] Wallis, A. E., Whitehead, J. C., Zhang, K. 2007. The removal of dichloromethane from atmospheric pressure air streams using plasma-assisted catalysis. Appl. Catal. B: Environ. 72 (2007), 282-288.

[11] H. H. Kim*, A. Ogata, S. Futamura. 2007. Complete Oxidation of Volatile Organic Compounds (VOCs) Using Plasma-Driven Catalysis and Oxygen Plasma. Int. J. PlasmaEnv. Sci. &Tech. Vol.1, No.1, (March 2007), p. 46-51.

[12] Martínez, H., Flores, O., Poveda, J. C., Campillo, B. 2012. Asphaltene Erosion Process in Air Plasma: Emission Spectroscopy and Surface Analysis for Air-Plasma Reactions. Plasma Sci. and Technol. 14 (4), 303-311.

[13] Martínez, H.,Yousif, F. B. 2008. Electrical and optical characterization of pulsed plasma of N_2-H_2.Eur. Phys. J. D, 46, 493-498.

[14] Riemann, K. U. 1997. The influence of collisions on the plasma sheath transition. Phys. Plasmas 4, 4158-4166.

[15] Pearse, R. W. B.,Gaydon, A. G. 1976. In The identification of molecular spectra, University Printing House Cambridge.

[16] Nakamura, J., Tsuji, M., Nakayama, A., Kawaguchi, A. 2008. Substrate-Controlled Reorganization of Solution-Grown Polyethylene Single Crystals through Partial Melting. Macromolecules 41, 1358-1363.

[17] Wyckoff, R. W. G. 1963. Crystal Structures. New York, IntersciencePubl1 (1963) repr. 1986.

[18] Sonoyama, N., Ezaki, K., Sakata, T. 2001. Continuous electrochemical decomposition of dichloromethane in aqueous solution using various column electrodes.Adv. in Environ. Research 6, 1 (Dec. 2001). 1-8.

[19] Ho, W., Barat, R. B.,Bozzelli, J. W. 1992. Thermal reactions of CH_2Cl_2 in H_2/O_2 mixtures: Implications for chlorine inhibition of CO conversion to CO_2.Combust. Flame 88, 3-4 (March 1992), 265-295.

[20] Janda, M., Martišovitš, V., Morvová, M., Machala, Z., Hensel, K. 2007.Monte Carlo simulations of electron dynamics in N_2/CO_2 mixturesEur. Phys. J. D 45 (2007), 309-315.